Consolidation of Rapidly Solidifying Al-6Si-0.3Cu Alloy by Spark Plasma Sintering and Cold Compaction Methods

Fatih YAŞAR[1], Fikret YILMAZ[2*]

[1]Faculty of Arts&Science, Department of Physics, TokatGaziosmanpasa University, Tokat, Turkey (fzyasar@gmail.com)
[2*]Faculty of Arts&Science, Department of Physics, TokatGaziosmanpasa University, Tokat, Turkey (fikretyilmaz79@gmail.com)

*Abstract –*In this study, Al-6Si-0.3Cu ribbon alloys produced by melt-spinning method were consolidated by two different methods, which are spark plasma sintering and cryogenic ball milling + cold compaction. From X-ray diffraction analysis, it was found that the solubility of Si in Al matrix in melt-spun alloys increased, but Si precipitated in SPS and ball milled+cold compacted alloys. Optical and scanning electron microscope observation revealed that while melt spun alloys have a very fine and homogenous microstructure, Si phase has become coarser in SPS and cold compacted alloys due to the sintering. The results showed that the spark plasma sintering method is a very effective method for compaction of melt-spun Al-6Si-0.3Cu alloy.

Citation: Yasar, F., Yilmaz, F. (2022). Consolidation of Rapidly Solidifying Al-6Si-0.3Cu Alloy by Spark Plasma Sintering and Cold Compaction Methods. International Journal of Multidisciplinary Studies and Innovative Technologies, x(x): xx-xx.

I. INTRODUCTION

Aluminum (Al) and its alloys with many unique properties have a wide range of uses. Aluminum alloys are particularly preferred in the packaging industry, as they are soft and ductile materials. The thin oxide layer formed on the surfaces increases the corrosion resistance of the alloy. Thanks to its high electrical and thermal conductivity, it is used in electronic applications. In addition, the strength/weight ratio of Al alloys is comparable to steel, making them the most preferred material in the aerospace and automotive industries [1-3].

Al-Si alloy with a silicon (Si) ratio of less than 12wt.% is called hypoeutectic Al alloys. This group of alloys is preferred in the automotive and marine industries due to their good fluidity, low thermal expansion coefficient, high corrosion resistance and high strength/weight ratio [4, 5]. Also, the absence of coarse primary Si phases in hypoeutectic Al-Si alloys increases the desired machinability, castability and weldability of the alloy, which makes it suitable for the construction of automotive engines, crankcases, cylinder blocks and pistons. The mechanical properties of hypoeutectic Al-Si alloys are dependent on the grain size, morphology and distribution of Si phase [6, 7]. It is also well known that the addition of trace amounts of copper (Cu) strengthens the Al-Si alloy and increases its ductility, which is explained by the formation of the Al_2Cu intermetallic compound [2].

Traditional casting techniques are mostly preferred in the production of commercial Al-Si alloys. In these techniques,

Si phases are dispersed as blocks in the microstructure due to the slow cooling rate and this affects the mechanical properties of the alloy negatively [8]. It is known from the literature that the mechanical properties of Al-Si alloys are greatly increased by eliminating these problems with rapid solidification techniques [9]. This technique is also effectively used in the production of shape memory alloys [10]. On the other hand, it is impossible to produce these alloys in the form of ingots, since at least one dimension of the rapidly solidified alloys is very small. In this respect, rapidly solidified alloys should be formed into ingot form by compaction methods in order to expand their application areas. Spark Plasma Sintering (SPS), which has been developed in recent years, is one of the most effective methods used in the compaction of powder materials [11]. The most important advantage of SPS is that it allows pressing and sintering to be done at the same time. Thus, the porosities that may occur in the material can be minimized.

In this study, Al-6wt% Si-0.3wt%Cu alloy was produced by melt-spinning method, which is a rapid solidification technique. Then, the produced melt-spun alloys were compacted via SPS and cold pressing techniques and examined in terms of microstructure and mechanical properties.

II. MATERIALS AND METHOD

High purity Al (99.9 %), Si (99.99 %) and Cu (99.9 %) were used to prepare the Al-6wt.%Si-0.3wt.%Cu master alloy. First of all, the alloy, which was prepared as 30 g, was

melted in the induction furnace. The alloy was melted in evacuated quartz crucible for 5 times to ensure both homogeneity and reduction of impurities (Figure 1a). The elemental composition of the master alloy was determined by X-ray Fluorescence (XRF, PANalytical-Epsilon5) and the results are listed in Table 1. As can be seen from the Table 1, the master alloy composition produced is very close to the initial composition.

Table 1. XRF results of Al-6Si-0.3Cu master alloy

Alloy	Al (wt.%)	Si (wt.%)	Cu (wt.%)	Other (wt.%)
Al-6Si-0.3Cu	93.359	6.040	0.382	0.219

Afterwards, the alloy was produced as ribbon with the melt spinning device (Edmund Bühler, MeltSpinner SC). The distance between the disc and nozzle was 2 mm, the disc rotation speed was 20 m/s and the injection pressure was set as 160 mbar. The ribbons with a thickness of 20 μm and a width of 1 cm were obtained (Figure 1b). For the spark plasma sintering (SPS) process, 1.5 g of melt-spun alloy was placed in a graphite crucible. The pellets were prepared by increasing the pressure value up to 300 kg/cm^2 with a ramp and the temperature value up to 450 ℃ and waiting for 10 minutes. The obtained pellets were then subjected to sintering at 560 ℃ for 10 hours in an argon environment in a high temperature furnace (Figure 1d).

A cryogenic ball milling device (Retch, CryoMill) was used to pulverize the ribbons (Figure 1c). The as-received powders were pressed with a cold pressing device under 300 kg/cm^2 pressures for 20 s and sintered at 560 ℃ for 10 hours in an argon atmosphere (Figure 1e).

The crystal structure of the alloys was analyzed by X-ray diffraction (PANalytical, Emperians) using CuKα monochromatic radiation in the range of 10-90 degrees. Microstructural analyzes were performed with conventional metal microscope and scanning electron microscope (SEM, QUANTA FEG 450). SEM images were taken in secondary electron (SE) and energy dispersive X-ray (EDX) mapping modes. Hardness analyzes were performed with Vickers hardness device (HighWood HWDM-3) under 300 g-f load and 10 s of dwell time under maximum load. Hardness values were calculated using the following equation;

$$HV = 1.854 \frac{P}{d^2} \tag{1}$$

where P is applied load and d is the average of the diagonal lengths of the indent.

Prior to hardness tests and microstructural analysis, the alloys were polished to 1 micron using standard metallography methods and then etched in 5% HF solution.

III. RESULTS AND DISCUSSION

X-ray diffraction (XRD) patterns of alloys are given in Figure 2. All possible diffraction peaks of Al (Ref. 98-005-3775) and Si (Ref. 98-004-3610) were observed in all alloys in the range of 2θ =10-90°. No peaks of Cu were found, which is explained by the dissolution of the element in the Al matrix. Very small SiO_2 peak was found in the XRD patterns

of the ball milled ribbons, which is due to the grinding environment (Figure 1c). In addition, a small amount of Al_2O_3 peak was observed in the sintered milled ribbon, which was formed by the oxidation of the alloy during sintering. (Figure 1d). It is seen that the peak intensity of the main Si peak decrease significantly in the melt-spun alloy (Figure 2b), which can be seen from the Si peak marked at an angle of 2θ=28.5°. This is due to the rapid cooling in melt-spun alloy increasing the solid solubility limits of Si in Al matrix, which is in agreement with the literature [12]. In the alloy produced by ball milling, the peak intensity of Si increased again, which can be explained by the precipitation of the Si dissolved in the Al matrix, due to the mechanical energy resulting from the collisions between the balls. Since sintering accelerates the precipitation mechanism of Si, the peak intensity increased more for sintered alloy (Figure 1d), which is in agreement with literature [13, 14].
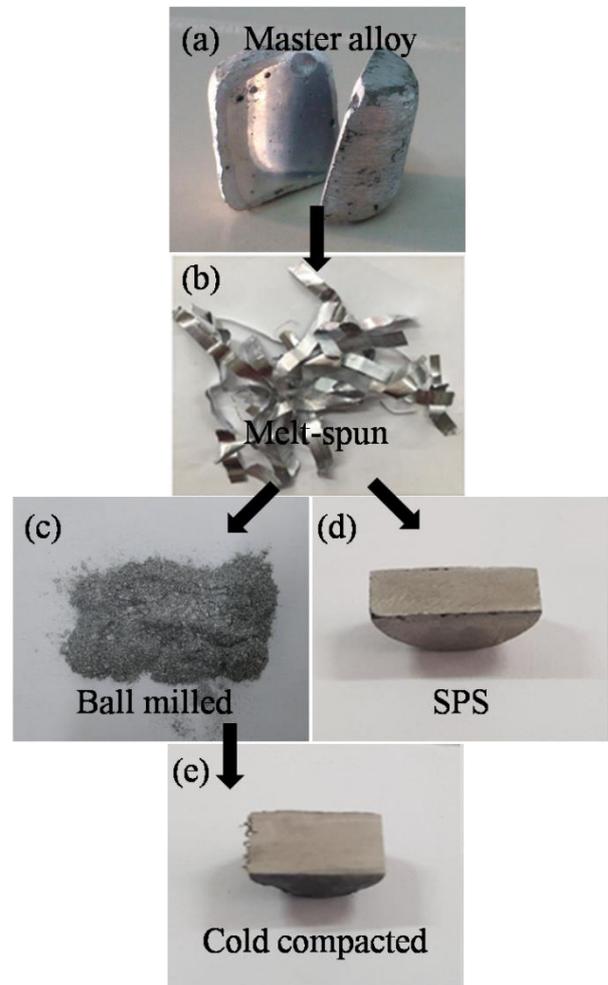
Fig. 1. The alloys produced by using (a) Induction furnace, (b) Melt spinning, (c) Cryogenic ball milling, (d) SPS+sintering from ribbons, (c) Cold compaction+Sintering from milled powders

In order to better understand the effects of rapid solidification, milling and sintering on the Al phase, the main peak belonging to the Al (111) plane is given in Figure 3. It can be seen that the peak of the melt-spun alloy shifts significantly to the lower angle, which can be explained with Bragg's law. According to the Bragg's law, the relation between diffraction angle and distance between crystalline planes is given;

$$n\lambda = 2dsin\theta \qquad\qquad (2)$$

where, n is the degree of diffraction, λ is the wavelength of the X-ray used, d is the distance between two planes, and θ is the diffraction angle. Shifting of the diffraction angle to the left side is due to the penetration of Si atoms into the crystal structure of Al as interstitial atoms during rapid solidification [15]. In addition, the increase in the peak width can be explained by the decrease in the crystal size of the alloy. The milling and sintering processes, as expected, caused Si atoms to ejection from the crystal structure of Al, and thus the diffraction angle shifted to the right again.
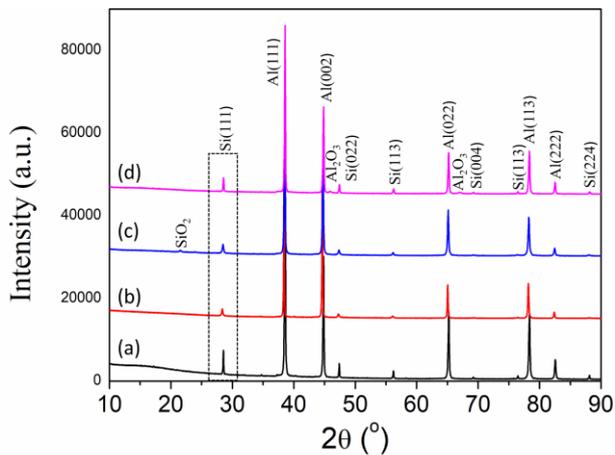
Figure 2. XRD patterns of the alloys, (a) Master alloy, (b) Melt-spun ribbon, (c) Ball milled ribbon, (d) Sintered ribbon
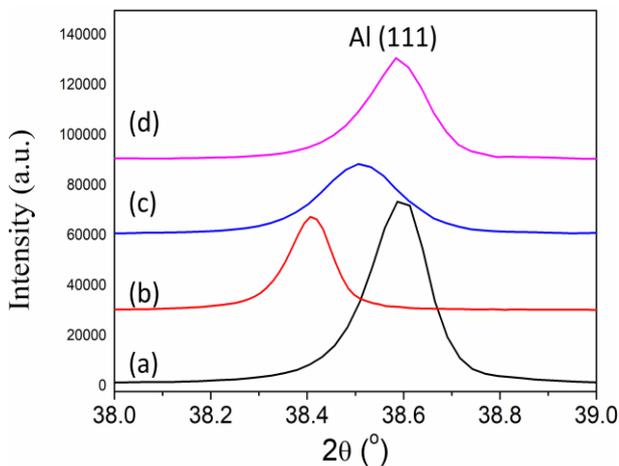
Figure 3. XRD peak of Al(111) plane of the alloys, (a) Master alloy, (b) Melt-spun ribbon, (c) Ball milled ribbon, (d) Sintered ribbon

Optical micrographs of the alloy are depicted in Figure 4. The microstructure of the master alloy consists of coarse eutectic Si and α-Al (Figure 4a). In melt-spun alloy, the microstructure was completely transformed into a fine and homogeneous structure (Figure 4b). The alloys produced SPS and milled+cold compacted also exhibit a homogeneous microstructure, but it is observed that Si has become coarser due to the effect of sintering (Figure 1c and d).

SEM images were taken to evaluate the microstructures of the alloys in more detail (Figure 5). It is seen that the master alloy consists of acicular eutectic Si and plate-like primary Si (Figure 5a). In melt-spun alloys, the microstructure consists of equiaxial and network-like α-Al phases and fine eutectic Si

phases. With the effect of rapid cooling, the dimensions of eutectic Si decreased from 50-100 micron to about 100-200 nanometres (measured with SemAfore software). In addition, the coarse morphology of the Si phase was modified to a fine fibrous structure (Figure 5b). In the SPS alloy, the eutectic Si is homogeneously dispersed in the Al matrix, but their size has become coarser and grown up to 1-5 microns. Compared with the SPS alloy, it was determined that the Si phase did not coarsen much in the ball milling + cold compacted alloy. It is also seen that the ribbon leaves are smaller in size in the cold compacted alloy. On the other hand, it is clearly seen that the gaps between the ribbon leaves are less in the SPS alloy than in the cold compacted alloy, which is related to simultaneous compaction and sintering in SPS alloy.
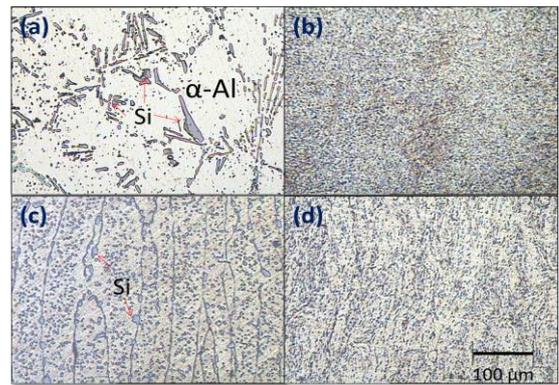
Figure 4. Optical micrographs of the alloys, (a) Master alloy, (b) Melt-spun ribbon, (c) SPS alloy, (d) Ball milled + Cold compacted alloy (Magnification: 200x)
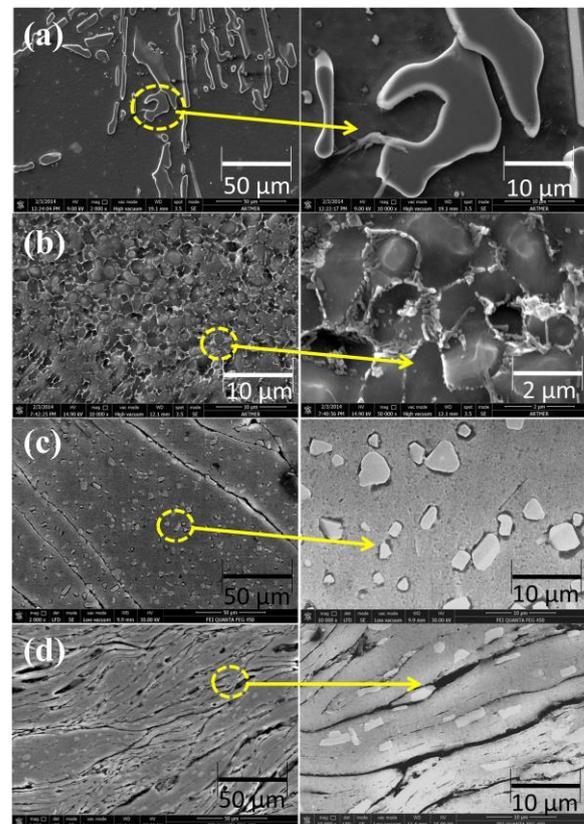
Figure 5. SEM images of the alloys, (a) Master alloy (Mag.: 2 and 10kx), (b) Melt-spun ribbon (Mag.: 10 and 50kx), (c) SPS alloy (Mag.: 2 and 10kx), (d) Ball milled + Cold compacted alloy (Mag.: 2 and 10kx)

Figure 6 shows Vickers hardness of the alloys. The hardness value of the master alloy (Bulk) was measured around 45 HV. The hardness value of the melt-spun alloy has increased (55 HV), which can be explained with a finer and homogeneous microstructure. The hardness value of the SPS alloy (52 HV) is higher than that of the bulk alloy, but decreased compared to that of the melt-spun alloy. This decrease can be explained by the coarsening of the Si phase. The hardness of milled+cold compacted alloy is the lowest among the alloys (38 HV). The reason for this may be that the bonding between the ribbon sheets is not formed well enough during sintering and thus the voids formed in the microstructure negatively affect the mechanical properties as shown in SEM images (Figure c and d).
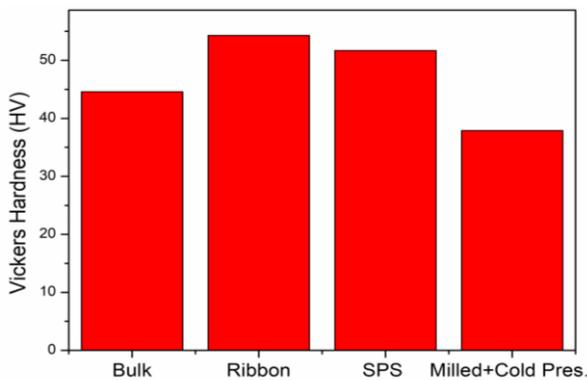
Figure 6 Vickers hardness of the alloys

IV. CONCLUSION

In this research, Al-6Si-0.3Cu alloy was successfully produced by induction melting and melt-spinning method, followed by SPS and ball milled+sintering method. The microstructure and mechanical properties of the produced alloys were compared. The most effective consolidation method was investigated by comparing the microstructure and mechanical properties of the alloys produced. In summary,

1. From XRD analyses, it was found that rapid solidification increases the solubility of Si in Al matrix. However, precipitation of Si was observed in SPS and cold compacted alloys due to sintering process.
2. Optical and SEM images revealed that master alloy consists of acicular eutectic Si and plate-like primary Si, while melt-spun alloy have homogenous microstructure and fine fibrous Si morphology. It was observed that the Si phase became coarser in SPS and cold compacted alloys.
3. From the hardness analysis, it was determined that the hardness value of the SPS alloy was between the master alloy and the melt-spun alloy, but the ball-milled + cold compacted alloy had the lowest hardness value.

When all the results are evaluated together, we believe that the SPS method is better than the ball milled + cold compacted method due to the short application time and sufficient mechanical properties.

Authors' Contributions
The authors' contributions to the paper are equal.

Statement of Conflicts of Interest

There is no conflict of interest between the authors.

Statement of Research and Publication Ethics

The authors declare that this study complies with Research and Publication Ethics

REFERENCES

[1] O. Uzun, F. Yilmaz, U. Kolemen, N. Basman, "Sb effect on micro structural and mechanical properties of rapidly solidified Al-12Si alloy", Journal of Alloys and Compounds, vol. 509, issue 1, pp. 21-26, 2011.
[2] C. Temiz, F. Yilmaz, U. Kolemen, "Investigation of microstructures and mechanical properties of Sc doped Al-5Cu alloys", Journal of the Faculty of Engineering and Architecture of Gazi University, vol. 37, issue 1, pp. 75-88, 2022.
[3] O. Uzun, F. Yilmaz, C. Emeksiz, S. Ergen, U. Kolemen, "Correlation of hardness and silicon morphology for Al-Si-Sb alloy", Archives of Metallurgy and Materials, vol. 63, issue 1, pp. 467-472, 2018.
[4] R. Oin, R.F. Yan, Z.P. Guan, G.Q. Zhang, J.W. Song, W. Ren, J.G. Wang, "Effect of vanadium on Fe-rich phase, mechanical properties and thermal conductivity of hypoeutectic Al–Si alloy", Materials Research Express, vol. 8, pp. 026518, 2021.
[5] F. Mao, Y. Qiao, P. Zhang, C. Chen, C. Zhang, "Modification mechanism of rare earth Eu on eutectic Si in hypoeutectic Al-Si alloy", vol. 16, issue 2, pp. 634-645, 2022.
[6] M.F. Kilicaslan, F. Yilmaz, S.J. Hong, O. Uzun, "Effect of Co on Si and Fe-containing intermetallic compounds (IMCs)in Al–20Si–5Fe alloys", Materials Science and Engineering A, vol. 556, pp. 716-721, 2012.
[7] W.K. Kang, F. Yılmaz, H.S. Kim, J.M. Koo, S.J. Hong, "Fabrication of Al–20 wt%Si powder using scrap Si by ultra-high-energymilling process", Journal of Alloys and Compounds, vol. 536S, pp. 45-49, 2012.
[8] W. Ding, L. Gou, L. Hu, H. Zhang, W. Zhao, J. Ma, J. Qiao, X. Li, "Modification of eutectic Si in hypoeutectic Al-Si alloy with novel Al-3Ti-4.35La master alloy", Journal of Alloys and Compounds, vol. 929, pp.167350, 2022.
[9] M.F. Kilicaslan, F. Yilmaz, S. Ergen, S.J. Hong, O. Uzun, "Microstructure and microhardness of melt-spun Al-25Si-5Fe-XCo (X=0, 1, 3, 5) alloys", Materials Characterization, vol. 77, pp. 15-22, 2013.
[10] S. Ergen, O. Uzun, F. Yilmaz, M.F. Kilicaslan, "Shape memory properties and microstructural evolution of rapidly solidified CuAlBe alloys", Materials Characterization, vol. 80, pp. 92-97, 2013.
[11] D. Yim, P. Sathiyamoorthi, S.J. Hong, H.S. Kim, "Fabrication and mechanical properties of TiC reinforced CoCrFeMnNi high-entropy alloy composite by water atomization and spark plasma sintering", vol. 781, pp. 389-396, 2019.
[12] Z. Chen, Y. Lei, H. Zhang, "Structure and properties of nanostructured A357 alloy produced by meltspinning compared with direct chill ingot", vol. 509, pp. 7473-7479, 2011.
[13] X. Zhang, L. Li, Z. Peng, J. Gao, "Microstructure and mechanical properties of an Al-11La-6Mgalloy prepared by the melt spinning and spark plasma sintering", Journal of Physics: Conference Series, vol. 2044, pp. 012099, 2021.
[14] E.M. Ahmet, M.R. Ebrahim, "Microstructure and microhardness evolution of melt-spunAl-Si-Cu alloy", The European Physical Journal Plus, vol. 129, pp. 60-68, 2014.
[15] E.M. Ahmed, "THE INFLUENCE OF RAPID SOLIDIFICATION ON THE PHYSICALPROPERTIES OF Al-Mn-Ce-Sb ALLOYS", Asian Journal of Physical Sciences, vol. 1, pp. 1-9, 2012.